Organic & Biomolecular Chemistry

Cite this: *Org. Biomol. Chem.*, 2012, **10**, 5410

www.rsc.org/obc

PAPER

A BODIPY-based colorimetric and fluorometric chemosensor for Hg(II) ions and its application to living cell imaging†

Mani Vedamalai and Shu-Pao Wu*

Received 20th March 2012, Accepted 30th May 2012
DOI: 10.1039/c2ob25589h

A new monostyryl boron dipyrromethene derivative (**MS1**) appended with two triazole units indicates the presence of Hg^{2+} among other metal ions with high selectivity by color change and red emission. Upon Hg^{2+} binding, the absorption band of **MS1** is blue-shifted by 29 nm due to the inhibition of the intramolecular charge transfer from the nitrogen to the BODIPY, resulting in a color change from blue to purple. Significant fluorescence enhancement is observed with **MS1** in the presence of Hg^{2+}; the metal ions Ag^{+}, Ca^{2+}, Cd^{2+}, Co^{2+}, Cu^{2+}, Fe^{2+}, Fe^{3+}, K^{+}, Mg^{2+}, Mn^{2+}, Ni^{2+}, Pb^{2+}, and Zn^{2+} cause only minor changes in the fluorescence of the system. The apparent association constant (K_a) of Hg^{2+} binding in **MS1** is found to be 1.864×10^5 M^{-1}. In addition, fluorescence microscopy experiments show that **MS1** can be used as a fluorescent probe for detecting Hg^{2+} in living cells.

Introduction

The development of chemosensors for detecting biologically and environmentally important metal ions, such as Cu^{2+}, Zn^{2+}, Hg^{2+}, and Pb^{2+}, has attracted much attention. Mercury is one of the most toxic heavy metal elements and exists in three forms: elemental, inorganic, and organic mercury. Mercury ions have high affinity for thiol groups in proteins, leading to the malfunction of cells and consequently causing many health problems in the brain, kidney, and central nervous system. Its accumulation in the body results in a wide variety of diseases, such as prenatal brain damage; serious cognitive and motion disorders; and Minamata disease.[1] In order to detect mercury ions in biological and environmental samples, the design of highly selective and sensitive mercury sensors has been an important issue.

In general, several traditional methods[2] for the detection of mercury ions in various samples have been developed, including atomic absorption–emission spectroscopy,[3] inductively coupled plasma mass spectroscopy (ICPMS),[4] and inductively coupled plasma–atomic emission spectrometry (ICP-AES).[5] Although these methods are quantitative, most of these methods require expensive instruments and are not good for on-site analysis. Recently, more attention has been focused on the development of fluorescent chemosensors for the detection of Hg^{2+} ions.[6]

Numerous molecular probes using different receptors and fluorescent units have been developed for Hg^{2+} detection. Because Hg^{2+} is known as a fluorescence quencher due to spin–orbit coupling,[7] most fluorescent chemosensors detect Hg^{2+} through a fluorescence quenching. Due to sensitivity concerns, fluorescent chemosensors detecting metal ions using fluorescence enhancement are more easily monitored than those using fluorescence quenching. This paper reports on a newly designed monostyryl boron dipyrromethene (BODIPY) based fluorescent enhancement Hg^{2+} chemosensor, based on intramolecular charge transfer (ICT). When Hg^{2+} binds to the chemosensor, it blocks the ICT mechanism, giving rise to a color change and fluorescence enhancement of BODIPY.

In this study, a monostyryl BODIPY-based fluorescent chemosensor (**MS1**) containing two triazole units was designed for metal ion detection (Scheme 1). **MS1** was blue and exhibits weak fluorescence. Binding metal ions to the chemosensor blocks the ICT mechanism and results in a color change and fluorescence enhancement of BODIPY. The metal ions Ag^{+}, Ca^{2+}, Cd^{2+}, Co^{2+}, Cu^{2+}, Fe^{2+}, Fe^{3+}, Hg^{2+}, K^{+}, Mg^{2+}, Mn^{2+}, Ni^{2+}, Pb^{2+}, and Zn^{2+} were tested for metal ion binding selectivity with **MS1**, but Hg^{2+} was the only ion that caused a red emission upon binding with **MS1**. The fluorescence microscopy experiments also demonstrated that **MS1** can be used as a fluorescent probe for detecting Hg^{2+} in living cells.

Result and discussion

Synthesis of MS1

The synthesis of the fluorescent probe, **MS1**, is outlined in Scheme 1. Mono formylated dipyrromethane (1) was

Department of Applied Chemistry, National Chiao Tung University, Hsinchu, Taiwan, Republic of China. E-mail: spwu@mail.nctu.edu.tw; Fax: +886-3-5723764; Tel: +886-3-5712121-ext56506

†Electronic supplementary information (ESI) available: ^1H and ^{13}C NMR spectra of compounds **2**, **3**, **4**, **5**, and **MS1**; ESI-MS of **MS1**–Hg^{2+}. See DOI: 10.1039/c2ob25589h

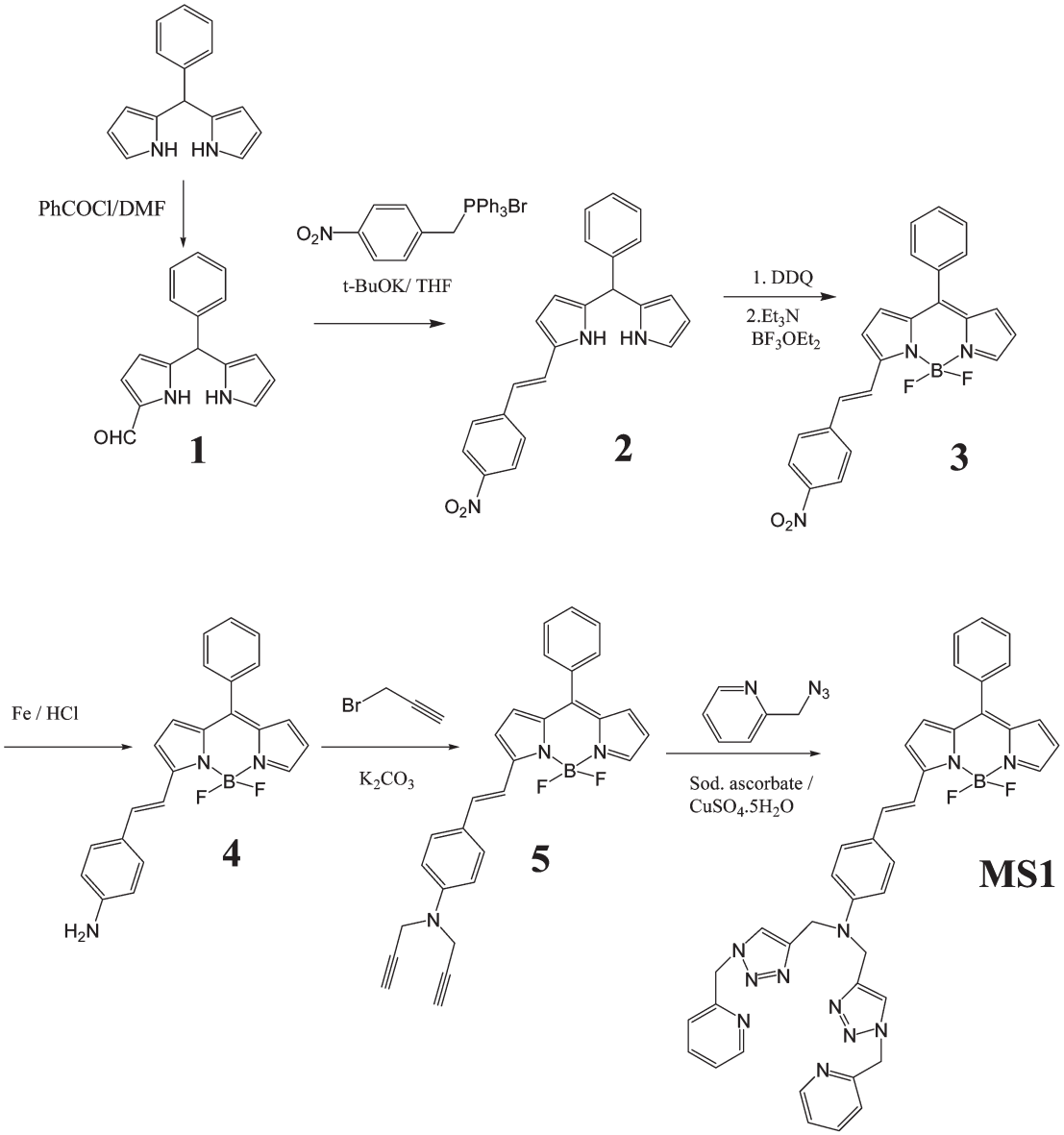

Scheme 1 Synthesis of **MS1**.

synthesized according to the procedure found in the literature.[9] Compound **2** was obtained by a Wittig reaction of (4-nitrobenzyl)triphenyl phosphonium bromide and mono formylated dipyrromethane to form a double bond between pyrrole and nitrobenzene. In the next step, compound **2** was transformed into a BODIPY skeleton by a stepwise reaction; first, dipyrromethane was oxidized to form dipyrromethene by DDQ, followed by dipyrromethene conversion into a BODIPY in the presence of boron trifluoride. Further reduction of compound **3** using iron powder gave compound **4**. The reaction of compound 4 with propargyl bromide in the presence of potassium carbonate yielded compound **5**. **MS1** was obtained by treatment of compound **5** with picolyl azide under click chemistry conditions. The absorption spectrum of **MS1** displays an absorption peak centered at 606 nm with a molar extinction coefficient of 6.2×10^4 M^{-1} cm^{-1}. The absorption maximum of **MS1** has about a 100 nm red shift in comparison to that of the standard BODIPY dye.[8] This red shift was assigned to a substitution of an amino styryl group at the "3" position of the BODIPY group.

Cation sensing selectivity

The sensing ability of **MS1** was tested by mixing it with metal ions Ag^+, Ca^{2+}, Cd^{2+}, Co^{2+}, Cu^{2+}, Fe^{2+}, Fe^{3+}, Hg^{2+}, K^+, Mg^{2+}, Mn^{2+}, Ni^{2+}, Pb^{2+}, and Zn^{2+}. Qualitatively, Hg^{2+} was the only ion that caused a visible color change (from blue to purple) and red fluorescence from **MS1** (Fig. 1). Other metal ions led to no significant change in the fluorescence of **MS1**. Quantitative absorption and fluorescence spectra of **MS1** were taken in the presence of several transition metal ions. Hg^{2+} was the only metal ion that caused a significant red emission (Fig. 2). During Hg^{2+} titration with **MS1**, the absorption band at 606 nm was shifted to 577 nm (Fig. 2). This caused a visible color change from blue to purple.

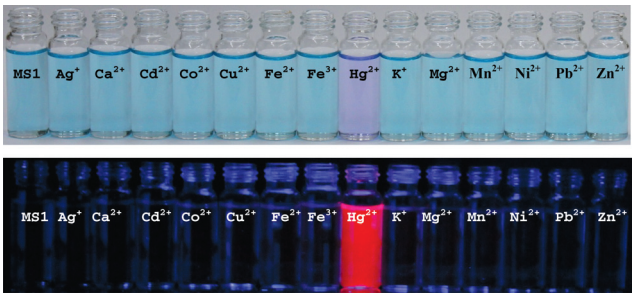

Fig. 1 Colorimetric change (top) and fluorescence change (bottom) of **MS1** (4 μM) with 60 μM of individual cations.

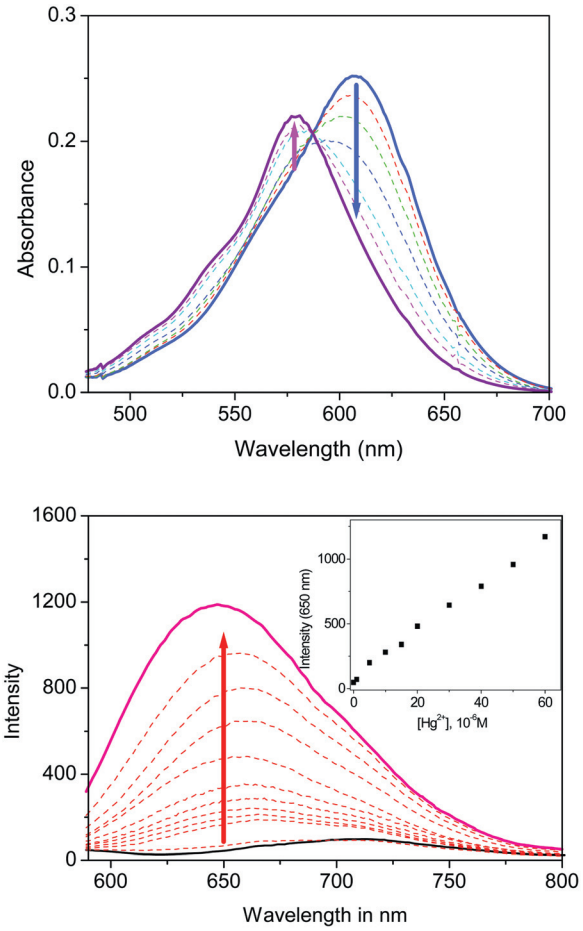

Fig. 2 Absorption (top) and emission (bottom) changes of chemosensor **MS1** (4 μM) in the presence of various equivalents of Hg^{2+} in acetonitrile–water (v/v = 9 : 1, 2.5 mM Hepes, pH 7.0) solutions.

During Hg^{2+} titration with **MS1**, a new emission band centered at 650 nm formed (Fig. 2). After adding 15 equivalents of Hg^{2+}, the quantum yield of the emission band was $\Phi = 0.327$, which is 65 fold higher than that of **MS1**, with $\Phi = 0.005$. These observations indicate that Hg^{2+} is the only metal ion that readily binds with **MS1**, causing significant fluorescence enhancement and permitting highly selective detection of Hg^{2+}.

To study the influence of other metal ions on Hg^{2+} binding with **MS1**, we performed competitive experiments in the presence of Hg^{2+} (60 μM) with other metal ions (150 μM) (Fig. 3).

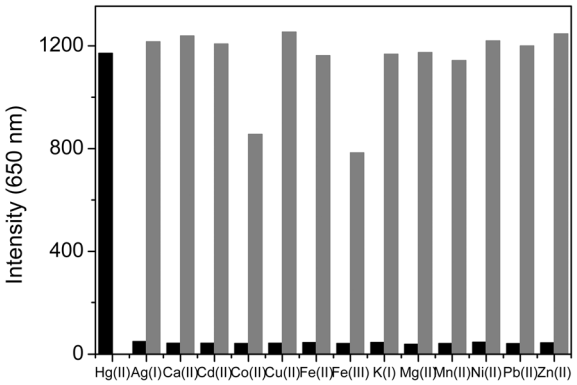

Fig. 3 Fluorescence response of **MS1** (4 μM) to the addition of Hg^{2+} (60 μM) or 150 μM of other metal ions (black bars) and to the mixture of other metal ions (150 μM) with 60 μM of Hg^{2+} (gray bars) in acetonitrile–water (v/v = 9/1, 2.5 mM Hepes, pH 7.0) solutions. The excitation wavelength is 550 nm.

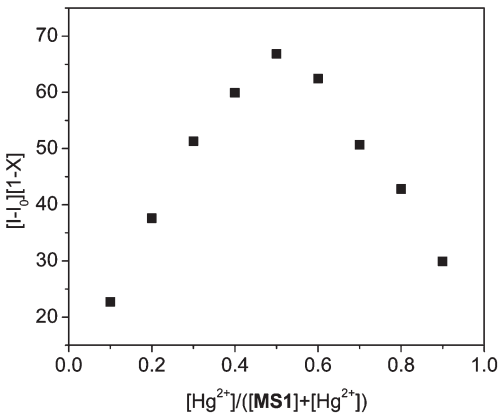

Fig. 4 Job plot of Hg^{2+}–**MS1** complexes in acetonitrile–water (v/v = 9 : 1, 2.5 mM Hepes, pH 7.0) solutions. The monitored wavelength was 650 nm. The total concentration of the sensor and Hg^{2+} ion was 8 μM.

Fluorescence enhancement caused by the mixture of Hg^{2+} with most metal ions was similar to that caused by Hg^{2+} alone. A smaller fluorescence enhancement was observed when Hg^{2+} was mixed with Co^{2+} or Fe^{3+}. This indicates that only Co^{2+} and Fe^{3+} compete with Hg^{2+} for binding with **MS1**. Most of the other metal ions do not interfere with the binding of **MS1** with Hg^{2+}.

In order to understand the binding stoichiometry of **MS1**–Hg^{2+} complexes, Job plot experiments were carried out. In Fig. 4, the emission intensity at 650 nm was plotted as a function of the mole fraction of **MS1** under a constant total concentration. Maximum emission intensity was reached when the mole fraction was 0.5. These results indicate a 1 : 1 ratio for **MS1**–Hg^{2+} complexes, in which one Hg^{2+} ion was bound with one **MS1**. Further, the formation of 1 : 1 **MS1**–Hg^{2+} complex was confirmed using ESI-MS in which the peak at *m*/*z* 929.9 indicates a 1 : 1 stoichiometry for **MS1**–Hg^{2+} complexes (see Fig. S11 in ESI†). The apparent association constant was calculated from Fig. 5 by using nonlinear regression analysis and was found to be 1.864×10^5 M^{-1}. The detection limit of **MS1** as a

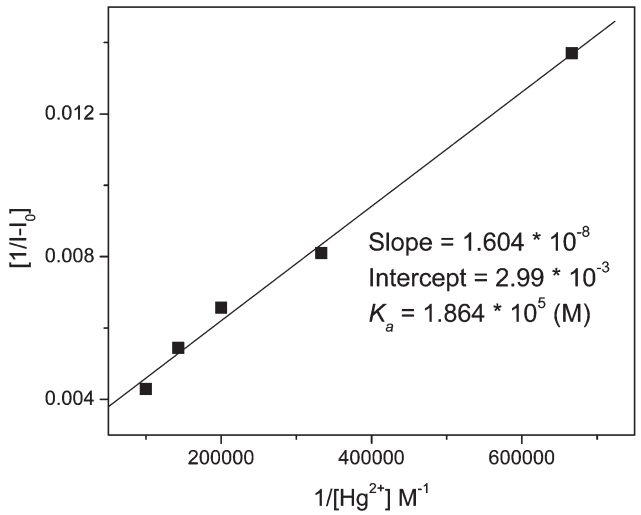

Fig. 5 Benesi-Hildebrand plot of the Hg^{2+}–**MS1** complexes in acetonitrile–water (v/v = 9 : 1, 2.5 mM Hepes, pH 7.0) solutions. The monitored emission wavelength was 650 nm.

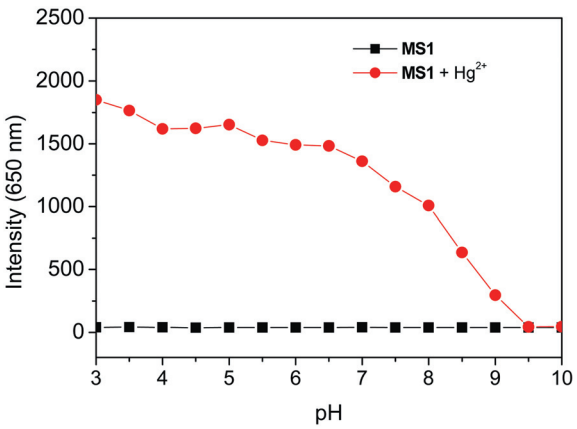

Fig. 6 Fluorescence intensity (650 nm) of **MS1** (4 μM) (■), and after addition of Hg^{2+} (60 μM) (●) in an acetonitrile–water (v/v = 9 : 1, 2.5 mM buffer) solution as a function of different pH values. The excitation wavelength was 550 nm.

fluorescent sensor for the analysis of Hg^{2+} was determined from the variation of fluorescence intensity as a function of the concentration of Hg^{2+} (see Fig. S12 in the ESI†). It was found that **MS1** has a detection limit of 0.226 μM, which allows micromolar concentrations of Hg^{2+} to be detected.

A pH titration of **MS1** was performed to investigate a suitable pH range for Hg^{2+} sensing. As depicted in Fig. 6, the emission intensities of metal-free **MS1** were very low. After mixing **MS1** with Hg^{2+}, the emission intensity at 650 nm remained a maximum in the pH range of 3.0–7.0. Above pH 7.5, the emission intensity decreased. This indicates poor stability of the **MS1**–Hg^{2+} complexes at high pH values.

To gain a clearer understanding of the structure of **MS1**–Hg^{2+} complexes, ^{1}H NMR spectroscopy (Fig. 7) was employed. Hg^{2+} is a heavy metal ion and can affect the proton signals that are close to Hg^{2+} binding.[9] In the ^{1}H NMR spectra of **MS1**, the proton (H_l, triazole) signal at 7.75 ppm showed down-field shifts upon the addition of Hg^{2+}. The down-field shifts upon Hg^{2+} coordination are due to a decrease in electron density induced by Hg^{2+}. This indicated that Hg^{2+} binding occurs mainly through the nitrogen at the triazole ring. The proton signals (H_j and H_k) showed up-field shifts upon the addition of Hg^{2+}. This indicated that Hg^{2+} binds to the amine attached to the phenyl ring and Hg^{2+} binding affects the ring current at the phenyl ring. The proton signals (H_n, H_o, H_p & H_q) at the pyridine were slightly influenced by Hg^{2+} binding. This showed weak interactions between Hg^{2+} and the pyridines. These observations revealed that Hg^{2+} binding with **MS1** was mainly through one amine at the phenyl ring and two nitrogens at two triazole units. Hg^{2+} also had weak interactions with two nitrogens at pyridine moieties.

Living cell imaging

MS1 was also applied to living cell imaging. For the detection of Hg^{2+} in living cells, HeLa cells were cultured in DMEM supplemented with 10% FBS at 37 °C and 5% CO_2. Cells were plated on 14 mm glass coverslips and allowed to adhere for 24 hours. HeLa cells were treated with 2 μM $Hg(BF_4)_2$ for 30 min and washed with PBS for three times. Then cells were incubated with **MS1** (2 μM) for 30 min and washed with PBS to remove the remaining sensor. The images of the HeLa cells were obtained using a fluorescence microscope. Fig. 8 shows the images of HeLa cells with **MS1** after the treatment of Hg^{2+}. The overlay of fluorescence and bright-field images reveal that the fluorescence signals are localized in the intracellular area, indicating a subcellular distribution of Hg^{2+} and good cell-membrane permeability of **MS1**.

Conclusions

In summary, the new fluorescence chemosensor **MS1** exhibits a high affinity and selectivity for Hg^{2+} ions over competing metal ions. Fluorescence was significantly enhanced by chemosensor **MS1** in the presence of Hg^{2+}, and the addition of Ag^+, Ca^{2+}, Cd^{2+}, Co^{2+}, Cu^{2+}, Fe^{2+}, Fe^{3+}, K^+, Mg^{2+}, Mn^{2+}, Ni^{2+}, Pb^{2+}, or Zn^{2+} barely affected the fluorescence. This BODIPY-based Hg^{2+} chemosensor also provides an effective method of Hg^{2+} sensing in living cell imaging.

Experimental section

General

All reagents were obtained from commercial sources and used as received without further purification. UV-vis spectra were recorded on an Agilent 8453 UV-vis spectrometer. Fluorescence spectra were recorded in a Hitachi F-4500 spectrometer.^{1}H and ^{13}C NMR spectra were recorded on a Bruker DRX-300 NMR Spectrometer, Varian AS500 Unity Innova Spectrometer and Varian VNMRS 600 NMR Spectrometer.

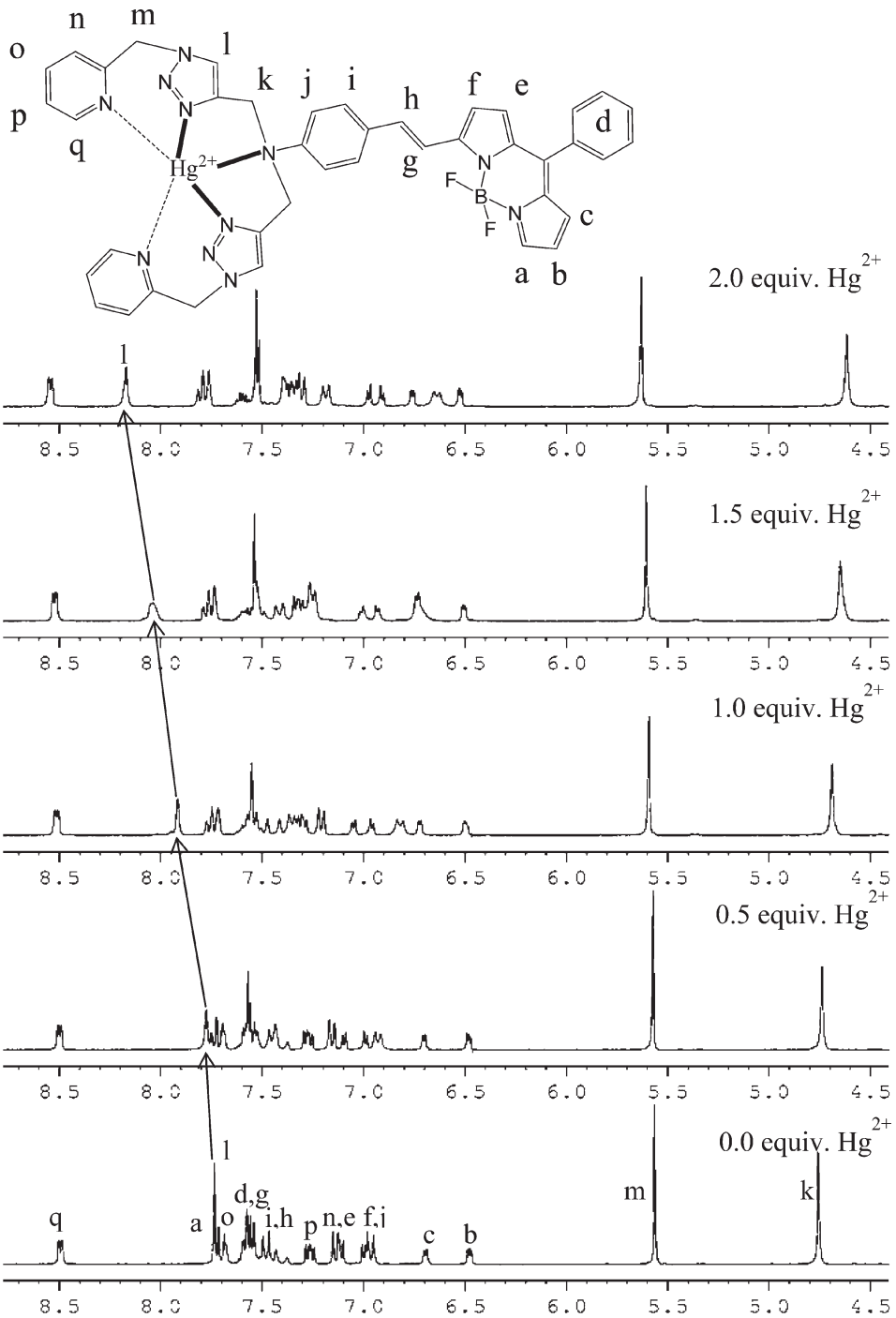

Fig. 7 ^{1}H NMR spectra of **MS1** (5 mM) in the presence of different concentrations of Hg^{2+} in CD_3CN.

Synthesis

Synthesis of 1-formyl-5-phenyldippyromethane (1). Compound **1** was obtained in modest yield by treating 5-phenyldipyrromethane with benzoyl chloride and DMF under dry N_2.[10]

Synthesis of 1-[2-(4-Nitro-phenyl)-vinyl]-5-phenyl-4,6-dipyrromethane (2). Potassium *tert*-butoxide (281 mg, 2.5 mmol) was added to a solution of (4-nitrobenzyl)triphenyl phosphonium bromide (1.002 g, 2.1 mmol) in dry THF (30 mL). The solution was stirred at room temperature for 30 min. Compound **1** (500.2 mg, 2 mmol) dissolved in dry THF (10 mL) was added dropwise to the mixture. The reaction mixture was heated at 66 °C for 12 h. Then solvents were removed under reduced pressure, and the crude product was purified by on column chromatography (hexane–ethyl acetate, 5 : 1) to give a compound **2** as a red solid. Yield: 70%, 517 mg. Melting point 163–164 °C. ^{1}H NMR (CD_3OD): δ = 8.14 (d, J = 9 Hz, 2H), 7.57 (d, J = 9 Hz, 2H), 7.17–7.31 (m, 6H), 6.80 (d, J = 16.5 Hz, 1H), 6.67 (dd, J = 1.5 Hz, 2.7 Hz, 1H), 6.33 (d, J = 3.6 Hz, 1H), 6.00

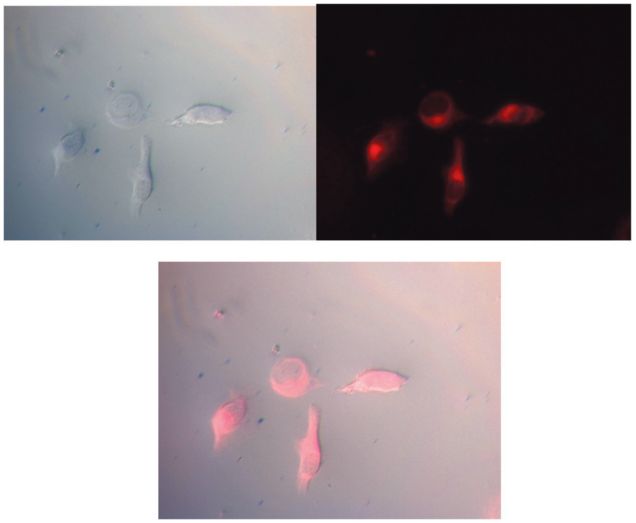

Fig. 8 Hg^{2+}-treated HeLa cell images. (Top left) Bright field image; (Top right) fluorescence image; and (Bottom) merged image.

(t, J = 3.0 Hz, 1H), 5.75 (d, J = 3.3 Hz, 1H), 5.73 (dd, J = 1.8 Hz, 2.1 Hz, 1H), 5.45 (s, 1H). ^{13}C NMR (CD_3OD): δ = 146.9, 146.7, 144.2, 139.0, 133.9, 131.4, 129.6, 129.2, 127.5, 126.7, 125.3, 125.0, 120.2, 118.2, 112.8, 110.3, 108.1, 107.8, 45.5. MS(FAB): m/z = 369. HRMS (FAB): calcd for $C_{23}H_{19}N_3O_4$: 369.1477; found 369.1481.

Synthesis of compound 3. 2,3-Dichloro-5,6-dicyano-1,4-benzoquinone (DDQ; 318 mg, 1.4 mmol) dissolved in CH_2Cl_2 (50 mL) was added to a solution of compound **2** (443 mg, 1.2 mmol) in CH_2Cl_2 (100 mL) under nitrogen, and the mixture was stirred for 1 h. It was then treated with Et_3N (3.0 mL) and $BF_3{\cdot}OEt_2$ (4.0 mL) for 3 h. The solvent was evaporated under reduced pressure, and the crude product was purified by column chromatography (ethyl acetate–hexane, 1 : 10) to give compound **3** as a pink solid. Yield 78%, 388.6 mg. Melting point 265–266 °C. ^{1}H NMR (CD_2Cl_2): δ = 8.24 (d, J = 8.7 Hz, 2H), 7.87 (s, 1H), 7.83 (d, J = 16.8 Hz, 1H), 7.76 (d, J = 9 Hz, 2H), 7.52–7.61 (m, 5H), 7.43 (d, J = 16.5 Hz, 1H), 7.04 (d, J = 4.5 Hz, 1H), 7.00 (d, J = 4.8 Hz, 1H), 6.90 (d, J = 3.9 Hz, 1H), 6.58 (d, J = 2.1 Hz, 1H). ^{13}C NMR (CD_2Cl_2): δ = 155.6, 148.1, 148.0, 145.0, 142.7, 142.6, 137.4, 135.2, 134.2, 132.5, 130.95, 130.90, 130.3, 128.8, 128.4, 124.5, 123.0, 118.5, 117.8. MS (EI): m/z (%) = 415 (100.0), 414 (30.1), 349 (8.4), 347 (10.4), 291 (5.1), 174 (4.8); HRMS (EI): calcd for $C_{23}H_{16}BF_2N_3O_4$ 415.1304; found: 415.1303.

Synthesis of compound 4. Iron powder (803.5 mg, 14.4 mmol) and water (4 mL) were added to a solution of compound **3** (373.6 mg, 0.9 mmol) in methanol (12 mL). It was then treated with HCl in methanol (6 mL, 0.5 mol L^{-1}). The reaction mixture was heated at 80 °C for 6 h. The reaction mixture was cooled to room temperature, and concentrated at reduced pressure. The crude product was purified by column chromatography (ethyl acetate–hexane, 1 : 3) to give a blue solid. Yield 80%, 277.3 mg). Melting point 238–239 °C. ^{1}H NMR (CD_2Cl_2): δ = 7.69 (s, 1H), 7.48–7.57 (m, 6H), 7.47 (d, J = 8.4 Hz, 2H), 7.40 (d, J = 16.2 Hz, 1H), 7.00 (d, J = 4.8 Hz, 1H), 6.97 (d, J = 4.8 Hz, 1H), 6.72 (d, J = 3.6 Hz, 1H), 6.70 (d, J = 8.4 Hz, 2H), 6.47 (dd, J = 1.8 Hz, 3.3 Hz, 1H), 4.10 (s, br, 2H). ^{13}C NMR (CD_2Cl_2): δ = 159.8, 149.5, 141.3, 140.9, 138.3, 137.5, 134.6, 134.1, 133.0, 130.8, 130.3, 130.2, 128.6, 126.5, 126.3, 118.3, 116.5, 115.1, 114.6. MS (EI): m/z (%) = 385 (100.0), 384 (30.1), 364 (20.6), 288 (4.1), 192 (4.8). HRMS (EI): calcd for $C_{23}H_{18}BF_2N_3$ 385.1562; found: 385.1559.

Synthesis of compound 5. Propargyl bromide (0.174 mL, 80% solution in toluene, 1.6 mmol) and potassium carbonate (276.4 mg, 2 mmol) were added to a solution of compound **4** (269.6 mg, 0.7 mmol) in acetone (5 mL). The reaction mixture was refluxed for two days. The solvent was evaporated under reduced pressure, and the crude product was purified by column chromatography (ethyl acetate–hexane, 1 : 5) to give compound **5** as a violet solid. Yield 87%, 281.5 mg. Melting point 156–157 °C. ^{1}H NMR (CD_3CN): δ = 7.76 (s, 1H), 7.49–7.67 (m, 9H), 7.16 (d, J = 4.8 Hz, 1H), 7.05 (d, J = 8.0 Hz, 1H), 7.01 (d, J = 9.0 Hz, 2H), 6.76 (d, J = 3.9 Hz, 1H), 6.53 (dd, J = 2.1 Hz, 3.9 Hz, 1H), 4.25 (d, J = 2.4 Hz, 4H), 2.56 (t, J = 2.4 Hz, 2H). ^{13}C NMR (CD_3CN): δ = 160.4, 149.7, 142.0, 141.8, 139.0, 137.9, 134.9, 134.5, 133.9, 131.4, 131.1, 130.3, 129.3, 127.2, 119.5, 118.3, 117.3, 115.4, 115.3, 79.9, 74.0, 40.8. MS (ESI): m/z = 462.1 $[M + H]^+$; HRMS (ESI): calcd $C_{29}H_{22}BF_2N_3$ $[M + H]^+$ 462.1953; found 462.1944.

Synthesis of MS1. Picolyl azide (160.9 mg, 1.2 mmol), $CuSO_4{\cdot}5H_2O$, (15.0 mg, 10 mol%), and sodium ascorbate (30.0 mg, 20 mol%) were added to a solution of compound **5** (277.3 mg, 0.6 mmol) in THF–H_2O (7 : 3, v/v; 15 mL) under nitrogen. The solution was stirred at room temperature for 12 h. A saturated ammonium chloride solution (20 mL) was added to the reaction mixture, and the organic phase was extracted with dichloromethane (100 mL, 3×). The combined organic extracts were dried with anhydrous $MgSO_4$. The solvent was evaporated under reduced pressure, and the crude product was purified by column chromatography (dichloromethane–methanol, 20 : 1) to give compound **MS1** as a dark violet solid. Yield 71%, 311.1 mg. Melting point 94–95 °C. ^{1}H NMR (CD_3CN): δ = 8.50 (d, J = 5.0 Hz, 2H), 7.76 (s, 2H), 7.69–7.72 (m, 3H), 7.40–7.59 (m, 9H), 7.26 (dd, J = 5.0 Hz, 7.0 Hz, 2H), 7.14 (d, J = 8.0 Hz, 2H), 7.06 (d, J = 5.0 Hz, 1H), 6.93–6.96 (m, 3H), 6.68 (d, J = 4.0 Hz, 1H), 6.48 (dd, J = 2.5 Hz, 3.8 Hz, 1H), 5.47 (s, 4H), 4.75 (s, 4H). ^{13}C NMR (CD_3CN): δ = 161.6, 156.6, 151.4, 151.2, 146.2, 143.2, 141.9, 139.0, 138.8, 138.7, 135.7, 135.1, 134.6, 132.1, 131.7, 131.3, 130.0, 127.2, 126.2, 125.2, 124.8, 123.7, 120.3, 118.9, 117.7, 114.9, 56.6, 47.6. MS (ESI): m/z = 730.2 $[M + H]^+$. HRMS (ESI): calcd for $C_{41}H_{34}BF_2N_{11}$ $[M + H]^+$ 730.3138; found 730.3146.

Determination of the binding stoichiometry and the apparent dissociation constants for the binding of Hg(II) to MS1

The binding stoichiometry of **MS1**–Hg^{2+} complexes was determined from a Job plot.[11] The fluorescence intensity at 650 nm

was plotted against the molar fraction of **MS1** with a total concentration of the sensor and Hg^{2+} ion of 8.0 μM. The molar fraction at maximum emission intensity represents the binding stoichiometry of the **MS1**–Hg^{2+} complexes. The maximum emission intensity was reached at a molar fraction of 0.5 (In Fig. 4). This result indicates that chemosensor **MS1** forms a 1 : 1 complex with Hg^{2+}. The apparent association constant (K_a) of **MS1**–Hg^{2+} complexes was determined by the Benesi-Hildebrand eqn (1)[12,13]

$$1/(F - F_0) = 1/\{K_a \times (F_{max} - F_0) \times [Hg^{2+}]\} + 1/(F_{max} - F_0), \quad (1)$$

where F is the fluorescence intensity at 650 nm at any given Hg^{2+} concentration, F_0 is the fluorescence intensity at 650 nm in the absence of Hg^{2+}, and F_{max} is the maxima fluorescence intensity at 650 nm in the presence of Hg^{2+} in solution. The association constant K_a was evaluated graphically by plotting $1/(F - F_0)$ against $1/[Hg^{2+}]$. Data were linearly fitted according to eqn (1) and the K_a value was obtained from the slope and intercept of the line.

Cell culture

The cell line HeLa was provided by the Food Industry Research and Development Institute (Taiwan). The HeLa cells were grown in DMEM (Dulbecco's modified Eagle's medium) supplemented with 10% FBS (fetal bovine serum) at 37 °C and 5% CO_2. Cells were plated on 14 mm glass coverslips and allowed to adhere for 24 hours.

Fluorescence imaging

Experiments to assess Hg^{2+} uptake were performed in PBS with 2 μM $Hg(ClO_4)_2$. Treat the cells with 4 μL of 1 mM metal ions (final concentration: 2 μM) dissolved in sterilized PBS (pH 7.4) and incubated for 30 min at 37 °C. The treated cells was washed PBS (3 × 2 mL) to remove remaining metal ions. Culture media (2 mL) was added to the cell culture, which was treated with a 10 mM solution of chemosensor **MS1** (4 μL; final concentration: 2 μM) dissolved in DMSO. The samples were incubated at 37 °C for 30 min. The culture media was removed, and the treated cells were washed with PBS (3 × 2 mL) before observation. Fluorescence imaging was performed with a ZEISS Axio Scope A1 Fluorescence Microscope. Cells loaded with **MS1** were excited at 545 nm using a lamp (Hg 50 W). Emission Filter was 570 nm.

Acknowledgements

We gratefully acknowledge the financial support of the National Science Council (ROC) and National Chiao Tung University.

Notes and references

1 (*a*) T. Takeuchi, N. Morikawa, H. Matsumoto and Y. Shiraishi, *Acta Neuropathol.*, 1962, **2**, 40–57; (*b*) M. Harada, *Crit. Rev. Toxicol.*, 1995, **25**, 1–24.

2 K. Leopold, M. Foulkes and P. Worsfold, *Anal. Chim. Acta*, 2010, **663**, 127–138.

3 (*a*) Y. Gao, S. De Galan, A. De Brauwere, W. Baeyens and M. Leermakers, *Talanta*, 2010, **82**, 1919–1923; (*b*) M. J. da Silva, A. P. S. Paim, M. F. Pimentel, M. L. Cervera and M. de la Guardia, *Anal. Chim. Acta*, 2010, **667**, 43–48.

4 (*a*) F. Moreno, T. Garcia-Barrera and J. L. Gomez-Ariza, *Analyst*, 2010, **135**, 2700–2705; (*b*) M. V. B. Krishna, K. Chandrasekaran and D. Karunasagar, *Talanta*, 2010, **81**, 462–472; (*c*) W. R. L. Cairns, M. Ranaldo, R. Hennebelle, C. Turetta, G. Capodaglio, C. F. Ferrari, A. Dommergue, P. Cescon and C. Barbante, *Anal. Chim. Acta*, 2008, **622**, 62–69.

5 X. Chai, X. Chang, Z. Hu, Q. He, Z. Tu and Z. Li, *Talanta*, 2010, **82**, 1791–1796.

6 (*a*) M. H. Lee, S. W. Lee, S. H. Kim, C. Kang and J. S. Kim, *Org. Lett.*, 2009, **11**, 2101–2104; (*b*) J. Fan, K. Guo, X. Peng, J. Du, J. Wang, S. Sun and H. Li, *Sens. Actuators, B*, 2009, **142**, 191–196; (*c*) V. Bhalla, R. Tejpal, M. J. Kumar and A. Sethi, *Inorg. Chem.*, 2009, **48**, 11677–11684; (*d*) K. G. Vaswani and M. D. Keranen, *Inorg. Chem.*, 2009, **48**, 5797–5800; (*e*) N. Wanichacheva, M. Siriprumpoonthum, A. Kamkaew and K. Grudpan, *Tetrahedron Lett.*, 2009, **50**, 1783–1786; (*f*) J. Du, J. Fan, X. Peng, P. Sun, J. Wang, H. Li and S. Sun, *Org. Lett.*, 2010, **12**, 476–479; (*g*) W. Shi, S. Sun, X. Li and H. Ma, *Inorg. Chem.*, 2010, **49**, 1206–1210; (*h*) S. Atilgan, T. Ozdemir and E. U. Akkaya, *Org. Lett.*, 2010, **12**, 4792–4795; (*i*) O. A. Bozdemir, R. Guliyev, O. Buyukcakir, S. Selcuk, S. Kolemen, G. Gulseren, T. Nalbantoglu, H. Boyaci and E. U. Akkaya, *J. Am. Chem. Soc.*, 2010, **132**, 8029–8036; (*j*) B. N. Ahamed and P. Ghosh, *Dalton Trans.*, 2011, **40**, 12540–12547; (*k*) F. Wang, S.-W. Nam, Z. Guo, S. Park and J. Yoon, *Sens. Actuators, B*, 2012, **161**, 948–953; (*l*) X. Ma, J. Wang, Q. Shan, Z. Tan, G. Wei, D. Wei and Y. Du, *Org. Lett.*, 2012, **14**, 820–823; (*m*) X. Jiang, C. Wong, P. Lo and D. K. P. Ng, *Dalton Trans.*, 2012, **41**, 1801–1807; (*n*) M. Vedamalai and S. Wu, *Eur. J. Org. Chem.*, 2012 (6), 1158–1163; (*o*) J. Dessingou, K. Tabbasum, A. Mitra, V. K. Hinge and C. P. Rao, *J. Org. Chem.*, 2012, **77**, 1406–1413; (*p*) B. Bag and B. Biswal, *Org. Biomol. Chem.*, 2012, **10**, 2733–2738.

7 D. S. McClure, *J. Chem. Phys.*, 1952, **20**, 682–686.

8 (*a*) W. Qin, T. Rohand, W. Dehaen, J. N. Clifford, K. Driesen, D. Beljonne, B. Van Averbeke, M. Van der Auweraer and N. Boens, *J. Phys. Chem. A*, 2007, **111**, 8588–8597; (*b*) A. Loudet and K. Burgess, *Chem. Rev.*, 2007, **107**, 4891–4932.

9 M. Kaupp, O. L. Malkina, V. G. Malkin and P. Pyykko, *Chem.–Eur. J.*, 1998, **4**, 118–126.

10 R. P. Brinnas and C. Bruckner, *Tetrahedron*, 2002, **58**, 4375–4381.

11 A. Senthilvelan, I. Ho, K. Chang, G. Lee, Y. Liu and W. Chung, *Chem.–Eur. J.*, 2009, **15**, 6152–6160.

12 H. A. Benesi and J. H. Hildebrand, *J. Am. Chem. Soc.*, 1949, **71**, 2703–2707.

13 R. B. Singh, S. Mahanta and N. Guchhait, *J. Mol. Struct.*, 2010, **963**, 92–97.

